ANALYSIS OF LUNAR BOULDER TRACKS: IMPLICATIONS FOR ROVER MOBILITY ON PYROCLASTIC DEPOSITS

V. T. Bickel[1,2], C. I. Honniball[3], S. N. Martinez[4], A. Rogaski[5], H. M. Sargeant[6], S. K. Bell[7], E. C. Czaplinski[8], B. E. Farrant[7], E. M. Harrington[9], G. D. Tolometti[9], and D. A. Kring[10,11], [1]Max Planck Institute for Solar System Research, Germany (bickel@mps.mpg.de), [2]ETH Zurich, Switzerland, [3]University of Hawai'i, United States, [4]Tulane University, United States, [5]South Dakota School of Mines & Technology, United States, [6]The Open University, United Kingdom, [7]University of Manchester, United Kingdom, [8]University of Arkansas, United States, [9]University of Western Ontario, Canada, [10]Lunar and Planetary Institute, Universities Space Research Association, United States, [11]NASA Solar System Exploration Research Virtual Institute, United States.

Introduction: In the context of long-term lunar exploration, Lunar Pyroclastic Deposits (LPDs) are high priority targets for scientific research and in situ resource utilization (ISRU). LPDs may host important volatiles such as OH and/or H2O that can be utilized for human exploration [1]; Surfaces of glassy material in LPDs may be enriched in Ag, Br, Cd, Cu, S, and Zn relative to their interiors [2-4]; Ilmenite and FeO-bearing LPDs can be reduced to produce oxygen for propellant as well as H_2O for consumption by crew [1]; LPDs can also be used to investigate the thermal and magmatic evolution of the lunar interior [5].

For scientific analysis and ISRU exploration, rovers need to access and successfully traverse these regions. However, knowledge about the geomechanical properties and overall trafficability of LPDs is limited. Incidents concerning rover mobility during the Apollo and Lunokhod missions highlight the importance of reliable estimates for the locomotion capabilities of rovers for future missions and, if required, adaptations in wheel and leg design for future missions in LPDs.

A fundamental aspect of trafficability is the bearing capacity of a soil; i.e., its ability to bear a rover. Here, bearing capacity of LPDs has been calculated using an analysis of boulder tracks in high-resolution satellite imagery (Narrow Angle Camera, NAC). Results have been compared with bearing capacities derived in highland and mare regions – terrains that have been successfully traversed in the past.

Methods: Boulder tracks are carved by rockfalls and are abundant on the Moon [6]. The relation between boulder dimensions, track dimensions, and soil properties defines the bearing capacity of the soil along the tracks. This work uses two equations to calculate bearing capacity, q_f, the first by Terzaghi [7]

$$q_f = 1.3cN_c + q_oN_q + 0.3\gamma_sBN_\gamma \quad (1)$$

and a variation of Hansen [8]:

$$q_f = cN_cs_cd_ci_cb_cg_c + q_oN_qs_qd_qi_qb_qg_q + 0.5\gamma_sBN_\gamma s_\gamma d_\gamma i_\gamma b_\gamma g_\gamma \quad (2)$$

with c as the cohesion of the soil, q_0 as the vertical stress within the soil, γ_s as the unit weight of the soil, B as footing width, and $N_{(c,q,\gamma)}$ as the bearing capacity factors that are based on the internal friction angle of the soil. Hansen introduces additional factors to better account for local topography and track orientation, which are the depth-, $d_{(c,q,\gamma)}$, the shape-, $s_{(c,q,\gamma)}$, the local slope inclination-, $g_{(c,q,\gamma)}$, the load inclination-, $i_{(c,q,\gamma)}$, and the foundation inclination factors, $b_{(c,q,\gamma)}$, respectively. Both equations consider a static case scenario, with Terzaghi assuming a circular contact area between boulder and soil, and Hansen assuming a rectangular contact area. The static condition is fulfilled as measurements are only performed close to the end of tracks, where the dynamic component of the boulder displacement is minimal.

NAC images containing 149 boulder tracks in LPD, highland, and mare regions were identified. Selected NAC images were processed with Isis3. Geometric measurements were performed in ArcGIS; i.e., boulder track width and depth, as well as the dimensions of the boulders themselves. Additional soil properties in specific examples of the terrains were retrieved or inferred from the literature based on Surveyor, Apollo, and Lunokhod data.

Results: A qualitative comparison of boulder tracks (Fig. 1) shows no significant difference among the regions, suggesting similar geomechanical properties. A quantitative analysis shows that q_f in maria and highlands is similar, while it is higher in LPD regions (Fig. 2). A two tail t-test confirms this observation, showing that LPDs have statistically equal or significantly higher q_f over the entire observed depth range from 0.19 to 5 m. Further, q_f in all regions increases with depth and decreases with increasing slope angle.

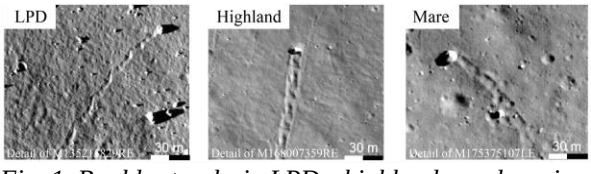

Fig. 1. Boulder tracks in LPDs, highlands, and maria.

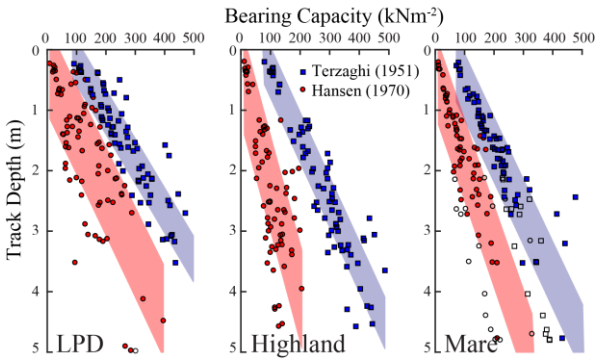

Fig. 2. q_f *over depth for all regions.*

Due to limitations in spatial resolution of the used sensor of about 0.5 m/pixel, tracks in the depth range from 0 to 0.19 m depth could not be resolved. For mare and highland regions, this sampling gap has been closed by calculating q_f of tracks carved by boulders, the LRV, and the MET, using images taken during the Apollo missions. All available data were used to derive a general bearing capacity distribution from the surface to a depth of 5 m depth in maria and highlands (Fig. 3). As LPDs feature statistically higher q_f than maria and highlands along the entire observed depth range, the same trend may be valid for the uppermost 19 cm of regolith in LPDs.

The general bearing capacity distribution is then used to estimate (Fig. 4) the sinkage, s, of wheeled rovers such as the Lunar Electric Rover (LER), Yutu-type and SandFlea-type rovers, of legged rovers such as the SpaceBok-type and the Spot-type, as well as of hybrids, such as RHex-type rovers. Variations in weight and wheel or leg dimensions have been considered using the rovers' effective wheel/foot contact area (A_{eff}) and weight:

$$s = mg_M / A_{eff} \quad (3)$$

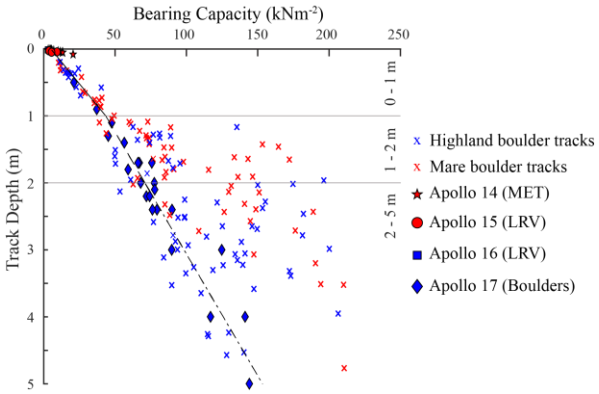

Fig. 3. Combination of q_f *values calculated with Hansen [8] for maria and highlands provides a conservative estimate for LPDs.*

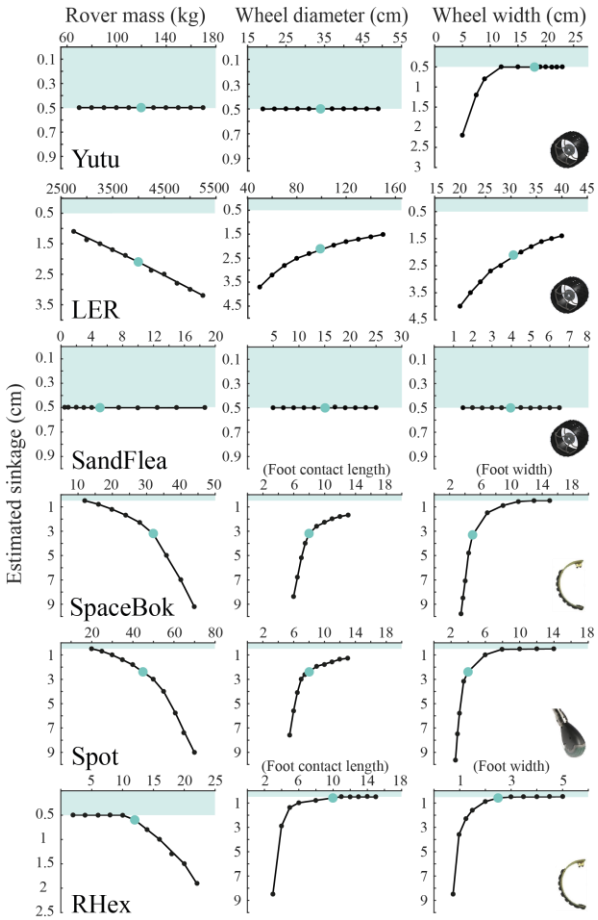

Fig. 4. Estimated rover sinkage in LPDs. Cyan point denotes sinkage using the default vehicle design specifications. Shaded area marks depth range from 0 – 0.5 cm, where sinkage has not been calculated.

Conclusions: The bearing capacity of LPDs may be equal or higher than that in mare and highland regions, implying sufficient trafficability and mobility for rovers. Estimated sinkage of various rover concepts in LPDs indicates that rover mobility can be efficiently ensured by maintaining sufficient wheel and foot widths. Additional weight due to increased payload and collected samples does not appear to be problematic. All findings remain to be confirmed in situ.

Acknowledgements: We thank USRA-LPI, CLSE, and NASA SSERVI for support.

References: [1] Allen C. et al. (1996) *JGR: Planets, 101(E11)*, 26085-26095. [2] Baedecker P. et al. (1974) *LPSC Proc.* [3] Chou C. (1975) *LPSC Proc., 6*, p. 137. [4] Wasson J. et al. (1976) *LSC Proc., 2*. [5] National Research Council (2007) *Nat. Ac. Pr.* [6] Kumar P. S. et al. (2016) *JGR: Planets 121*, 147–179. [7] Terzaghi K. (1951) *Chapman And Hall, Limited.; London*. [8] Hansen J. (1970) *Bulletin No. 11, DGI.*